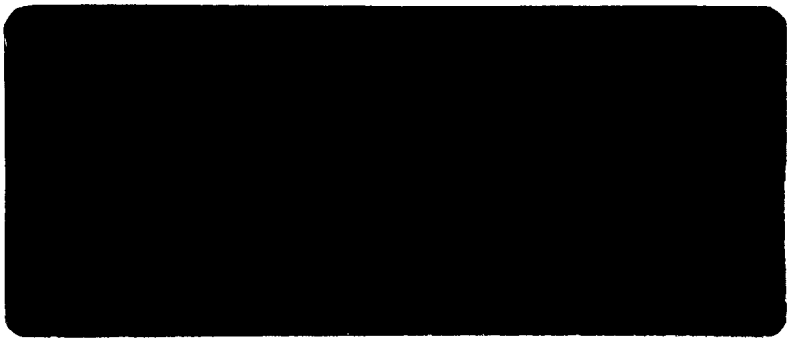

JET PROPULSION LABORATORY
CALIFORNIA INSTITUTE OF TECHNOLOGY
PASADENA, CALIFORNIA

NATIONAL AERONAUTICS AND SPACE ADMINISTRATION
CONTRACT NO. NASw-6

Technical Release No. 34-100

THE CRYOGENIC GYRO

John T. Harding
Robert H. Tuffias

JET PROPULSION LABORATORY
A RESEARCH FACILITY OF
NATIONAL AERONAUTICS
AND SPACE ADMINISTRATION
OPERATED BY
CALIFORNIA INSTITUTE OF TECHNOLOGY
PASADENA, CALIFORNIA

August 1, 1960

CONTENTS

FIGURES

FIGURES (Cont'd)

TABLES

Technical Release No. 34-100

THE CRYOGENIC GYRO[1]

John T. Harding
Robert H. Tuffias

ABSTRACT

The torqueless suspension of a superconducting sphere is made possible by the fact that the Meissner effect requires that magnetic forces on a superconductor are exerted normal to its surface. Furthermore, the lack of resistance allows high rotational speeds without eddy-current drag.

This paper discusses the results of theoretical and experimental studies on the behavior of a superconducting sphere suspended by a magnetic field.

[1]This paper presents the results of one phase of research carried out at the Jet Propulsion Laboratory, California Institute of Technology, under Contract No. NASw-6, sponsored by the National Aeronautics and Space Administration.

I. INTRODUCTION

The development of inertial guidance systems depends on the finding of methods to eliminate all unpredictable forces from the inertial element. In the gyro field, engineering techniques have been pushed almost to the limit in the design of mechanical rotor supports that minimize friction. A promising alternative to mechanical suspension is the use of the pressures exerted by electromagnetic fields.

A well-known example of field levitation is the lifting of a piece of iron by a magnet. Not so well known are three other, recently developed, levitation schemes:

1. The suspension of conductors by dc electric fields, or electrostatic support.
2. The suspension of non-ferrous metals by high-frequency magnetic fields.
3. The suspension of superconductors by dc magnetic fields.

All of these techniques have possible gyroscopic applications. Despite the constraints imposed by the fact that superconductivity is a cryogenic phenomenon, JPL engineers are investigating the superconducting gyro because it offers several significant advantages:

1. Superconductors, being diamagnetic, are repelled rather than attracted by sources of magnetic field. This feature makes possible an inherently stable support, unlike ferromagnetic or electrostatic suspensions which require feedback systems.
2. The dc current required for support can be trapped in a superconducting circuit, eliminating support power.

3. Maximum pressures, as limited by critical fields or breakdown fields, are higher for magnetic than for electric field supports.
4. Dimensional instability, a major contributor to the degredation of gyro performance, is virtually eliminated in materials at low temperatures where expansion coefficients approach zero.

To understand fully the principle of a magnetically supported superconductor, it is necessary to be aware of two properties of superconductors:

1. The vanishing of all resistance to the passage of electricity, which implies the absence of electric fields within a superconductor.
2. The exclusion of magnetic flux from the interior of a superconductor. This is known as the Meissner effect (Ref. 1) and it corresponds to complete diamagnetism.

The boundary condition imposed by the Meissner effect is that the normal component of the magnetic field vanishes at the superconducting surface. The magnetic force due to a field $\vec{B}$ on an element of surface $d\vec{S}$ is given by

$$\vec{dF} = \frac{\vec{B}}{\mu_0} (\vec{B} \cdot \vec{dS}) - \frac{B^2}{2\mu_0} \vec{dS} \qquad (1)$$

Thus the first term on the right vanishes for a superconductor with the result that the magnetic stress or pressure is normal to the surface. If the surface is a perfect sphere, all forces pass through the center of mass and no torques are possible, regardless of the ambient or applied external fields. Furthermore, the absence of resistivity makes possible rotation of the sphere without the eddy-current drag associated with conductors moving through magnetic fields.

In 1952, Ivan Simon, of the Arthur D. Little Company, (Ref. 2 and 3) showed that a hollow lead sphere immersed in liquid helium could be lifted stably by a two-coil support.

An independent analysis by Culver and Davis of the RAND Corporation, in 1956, (Ref. 4) showed that the cryogenic gyro indicated great promise as an accurate inertial guidance element. The Jet Propulsion Laboratory has undertaken a research and development program to transform Simon's basic superconducting suspension into the practical inertial guidance element envisaged by Culver and Davis.

II. DESIGN CONSIDERATIONS

The design of a cryogenic gyro can be catagorized into six parts:

1. Rotor - material selection and fabrication
2. Supporting field configuration
3. Spin-up
4. Read-out
5. Damping rotor vibration
6. Maintenance at cryogenic temperatures

The first and major effort to date has been to analyze the extent to which an actual coil system can be made to realize optimum design characteristics. Figure 1 shows the field plot for the simplest case, a single-coil and sphere configuration. Two things should be noted: the field lines do not enter the ball, and there are regions of high field density. A very important design characteristic is found in the minimization of the magnetic fields at the rotor surface -- this reduces the possibility of

exceeding the critical field strength of the superconductor, and of consequent breakdown.[2]

III. COMPUTER PROGRAMS

Two IBM 704 computer programs have been developed to analyze the problem of accomplishing these design characteristics. Fortunately, the case of a perfectly diamagnetic sphere in a magnetic field has particularly simple boundary conditions. For a coaxial array of current-carrying coils with the sphere on-axis, the answer can be found in terms of an image solution.

The location of the image coil is simply the "inversion" of the real coil with respect to the sphere. The strength of the image coil is greater than the strength of the real coil by the ratio of the distance of the real coil from sphere center to the radius of sphere. Proof that this construction satisfies the boundary conditions is given in Appendix A. Given the geometry and coil strengths of any number of co-axial coils, the program supplies the image currents, computes and plots the resulting field on and near the sphere surfaces. The magnetic force is computed by Eq. 1.

The case of an off-axis sphere in an equal array of coils is not as easy. It requires the expansion of the scalar potential for the induced field in spherical harmonics:

$$B = - \nabla \Phi$$

[2]Superconductivity is destroyed by either raising the temperature above the transition temperature or by subjecting the superconductor to a field greater than a limiting field - called the critical field. The critical field is a function of the temperature and the material.

where:

$$\Phi = \sum_{nm} \frac{a_{nm}}{r(n+1)} P_n^m (\cos\theta) \cos m\phi$$

r is measured from the sphere center, θ is the co-latitude angle measured from the field axis, ϕ is the longitude angle measured from the off-axis displacement direction; the a_{nm}'s being chosen to satisfy the boundary condition that no field can penetrate the sphere. This requires:

$$a_{nm} = - \frac{R^{n+2}}{(n+1)(1+\delta_m^0)2\pi} \frac{(2n+1)}{} \frac{(n-m)!}{(n+m)!} \int\int B_n P_n^m (\cos\theta) \cos m\phi \, d\cos\theta \, d\phi$$

where B_n is the normal component of the applied field.

Thus, once the a_{nm}'s are determined, the induced field is calculated and then added to the applied field to yield the total field at the surface of the sphere.

The magnetic force on the sphere is the integral of the Maxwell stress tensor (or magnetic pressure) over the surface of the sphere:

$$\vec{F} = \frac{-1}{2\mu_0} \int\int B^2 \, d\vec{S}$$

the components of which furnish the axial and radial forces on the sphere.

IV. ANALYTICAL RESULTS

A. Single-Coil Configurations

The simplest case, a single-coil and sphere, was analyzed to determine the optimum configuration with emphasis placed on the reduction of the maximum field

(B_{max}) on the surface of the sphere for a given lifting force. By varying the values a and α (Fig. 2a), the configuration characterized by the coil-radius to sphere-radius ratio (r_c/r_s) equal to 1.8 and the elevation to coil-radius ratio (z/r_c) equal to 1.4, is found to produce a minimum B_{max}. Figure 2b shows the curve of B_{max} versus elevation for a constant lifting force (obtained by varying the coil current). Figure 2c shows the curve of axial force versus elevation for a constant coil current. It can be seen that the transition between axial stability and instability occurs at z/r_c equal to 0.436. Figure 3 shows the curve of the ratio of the radial force to the axial force versus elevation when the sphere has a radial displacement of (a) 0.01 cm, or (b) 0.50 cm from the axis of the coil. From the figure it can be seen that the sphere is radially stable from $z/r_c = 0.435$ to $z/r_c = 0.767$ ($z/r_c < 0.435$ was not investigated). The radial force tending to return the ball to the axis is approximately 42 times as great when the sphere is moved 50 times further (from 0.01 cm to 0.50 cm) from the center at $z/r_c = 0.435$. Therefore, the sphere is stable, both axially and radially, and from $z/r_c = 0.435$ to $z/r_c = 0.767$.

B. Multi-Coil Configurations

In addition to the aforementioned criteria, it is also necessary to stabilize the rotor against high accelerations in all directions, which implies a spherically symmetric force field.

In designing a symmetrical multi-coil system, the only variable is current density. The additional constraints include a high maximum force and the ability of the system to absorb transient acceleration forces. No constraints were added with

regard to the readout (i.e., no gap constraints). The factors affecting current density are:

1. Direction of current flow.
2. Coil and sphere geometry (i.e., the distribution of coils about the sphere and gap size).
3. Current and coil geometry relationship.

To determine the optimum current direction, an eight-coil system (see Fig. 4) was analyzed under these three conditions:

1. Current flowing in the same direction in all the coils.
2. Current flowing in opposite directions in alternate coils.
3. Current flowing in the same direction in the upper four coils and in the opposite direction in the lower four coils.

From the computer program it was found that the eight-coil configuration was radially unstable under the first condition, was stable both axially and radially under the second and third conditions, but under the third condition produced a lower maximum field than under the second.

In evaluating the systems with regard to maximum force and energy absorption, a maximum-force term was used. It was computed by increasing the current until the maximum field became equal to the critical field.

The number of coils and the coil-sphere diameter (with equal angular spacing) were varied (equal current in each coil) with the results that led to the following conclusions:

1. Six coils are effectively equal to an infinite number of coils.

2. The optimum ratio of the coil-sphere diameter to rotor diameter, with respect to maximum force is 2.0.

Figure 5 shows the force-versus-position curves for an six-coil configuration when the coil-sphere diameter to rotor diameter ratios are 1.5, 2.0 and 4.0. Figure 6 shows the field plot for a six-coil configuration.

Analyses with respect to the current and coil geometry relationship reveal that symmetrical stability can be obtained by having the current in the equatorial coils greater than the current in the polar coils.

V. EXPERIMENTAL METHODS

A method utilizing the diagram of Fig. 7 was devised to trap current into a superconducting loop. Its operation is as follows:

1. The dc power supply is set at the required current level. Since Branch A has less inductance than Branch B, almost all of the current flows through Branch A.
2. The destruct coil is supplied with enough current so that its field exceeds the critical field of the superconducting wire it encloses. This wire then becomes normal, which greatly increases the resistance of Branch A. Branch B, therefore, carries almost all of the current.
3. The destruct coil is turned off, allowing Branch A to once again become superconducting. The current flowing in Branch B then flows through the circuit formed by A and B, since A and B are both superconducting and have infinitely less resistance than the copper leads.

4. The dc power supply is turned off and the current continues to flow through the circuit formed by A and B. The current in the superconducting loop is measured by using the readout coil. When the current in the superconducting circuit is destroyed, it induces an instantaneous current in the readout coil which can be read on a galvanometer.

Tests were performed to determine a method of making superconducting niobium joints. It was found that spot welding niobium, using high power, low pressure and short time durations (12 milliseconds for 1/32-in. diameter niobium wire) produced joints which were 85% as good as solid niobium wire (the joints broke down at 85% of the critical field).

Tests were performed on superconducting transformers which indicated that ideal loss-less transformers could be utilized for high-current applications.

Superconducting rotors for the experiments were made of either solid niobium or lead-plated sapphire, plastic, aluminum, or magnesium spheres. The spheres were plated either by electrochemical deposition or vacuum deposition. Tests have indicated that these methods can be refined to produce properties similar to the parent material.

VI. EXPERIMENTAL ANALYSIS

A. Computer Program Correlation

The initial experimental verification of the computer program was performed with the optimum single coil discussed previously and a lead-coated sphere. The

sphere was contained in a glass tube to prevent horizontal displacement. The curve of current-versus-elevation, shown in Fig. 8, shows the comparison between the experimental results and the analytical results. From this curve it can be seen that the experimental results agree with the analytical results within 5% in most cases, and with a maximum variation of 10%.

Figure 9 shows a 3.81 cm diameter lead-coated sphere stably supported by a single coil. Approximately 1000 ampere-turns were required to levitate the 8-gm sphere. The levitating current was trapped into the superconducting loop and remained constant for approximately 5 1/2 hours, during which time no measurable change in the elevation of the sphere was evident. This experiment also verified the computer results that a single coil could produce both horizontal and vertical stability, which previously had been thought to be impossible.

An experimental verification of both the on-axis and off-axis computer programs was made using the apparatus shown in Fig. 10. A solid niobium sphere was levitated using a two-coil unsymmetrical configuration. The coils were then rotated about a radial axis to obtain various off-axis stable positions. The current was measured and the ball position photographed to obtain the data. Figure 11 shows the on-axis comparison between the analytical and experimental results. As can be seen, all points except one are within 5% difference.

Table 1, which presents the tabulated data used with Fig. 12, shows the off-axis comparison. These results show differences ranging from 20 to 60%. These errors can be almost entirely attributed to measuring error. For example, in test No. 5, the linear measurement is only accurate to between .01 and .02 cm. If the

horizontal displacement (A) is increased by .015 cm the force ratio (F_r/F_z) becomes 0.48, reducing the difference to 17%. This can be accounted for by errors in angular measurement, distortion caused by the glass and liquid of the dewar system, and trapped flux in the sphere.

B. Levitation in a Vacuum

A solid niobium sphere was levitated in a vacuum as shown in Fig. 13. The sphere was located inside a tube which could be evacuated. The two-coil levitating configuration was located outside the tube in the liquid helium. To reduce the heat flow into the tube, radiation shields were used. The sphere was levitated in helium gas at 4.2° K and then the tube was evacuated. A minimum pressure of 2×10^{-6} mm of mercury was obtained during the levitation. No heating effects were evident during the levitation period of approximately two hours.

VII. CONCLUSIONS

With answers in sight to the problems of magnetic field support configuration, operation in a vacuum, and readout, the ultimate success of the cryogenic gyro appears to depend on the development of a rotor with the necessary spherical symmetry in regard to its mechanical and diamagnetic properties. This involves problems beyond the state of the art and requires pioneering materials research.

APPENDIX A

Appendix A offers proof that a current loop images itself in a diamagnetic sphere, as illustrated in Fig. A-1. The normal field at the surface of the sphere is given by Ref. 5, Eq. 6 and 7 of Section 7.12 and Eq. 3 of Section 7.13.

$$B_r \text{ real} = \frac{\mu I_r \sin\alpha}{2a_0} \sum_{n=1}^{\infty} \left(\frac{r}{a_0}\right)^{n-1} P_n^1(\cos\alpha)\, P_n(\cos\theta) \tag{A-1}$$

$$B_r \text{ image} = \frac{\mu I_i \sin\alpha}{2r} \sum_{n=1}^{\infty} \left(\frac{a_i}{r}\right)^{n-1} P_n^1(\cos\alpha)\, P_n(\cos\theta) \tag{A-2}$$

$$B_r = B_r \text{ real} + B_r \text{ image} = \frac{\mu}{2} \sin\alpha \sum_{n=1}^{\infty} P_n^1(\cos\alpha)\, P_n(\cos\theta)$$

$$\times \frac{r^{n-1}}{a_0^n} I_r + \frac{(a_i)^{n+1}}{r^{n+2}} I_i \tag{A-3}$$

$$B_r = 0 \text{ if } I_i = \frac{r^{2n+1}}{a_0^n (a_i)^{n+1}} I_r = \left(\frac{r^2}{a_0 a_i}\right)^{n+1} \frac{a_0}{r} I_r \tag{A-4}$$

Since I_i cannot depend on n, B_r vanishes for $a_i = r^2/a_0$ and $I_i = (a_0/r)(I_r)$.

REFERENCES

1. Jet Propulsion Laboratory, California Institute of Technology. Astronautics Information Literature Search No. 149, "Meissner Effect, Penetration Depth and Residual Magnetism in Superconductors," J. Hayes and E. Pereira, compilors, Pasadena, Calif.,

2. Simon, I. "Forces Acting on Superconductors in Magnetic Fields," Journal of Applied Physics, Vol. 24, No. 1 (January 1953), pp. 19-24.

3. Simon, I. "Frictionless Supports Uitlizing Electromagnetic Properties of Superconductors," Paper No. 54-33-4, presented at the First International Congress and Exposition of the Instrument Society of America, Philadelphia, Pa., September, 1954.

4. RAND Corporation. "An Application of Superconductivity to Inertial Navigation" by W. H. Culver and M. H. Davis. Santa Monica, Calif., RAND, January 7, 1957 (RM-1852).

5. Smythe, W. R. "Static and Dynamic Electricity," 2nd ed., pp. 273-275, McGraw Hill, New York, 1950.

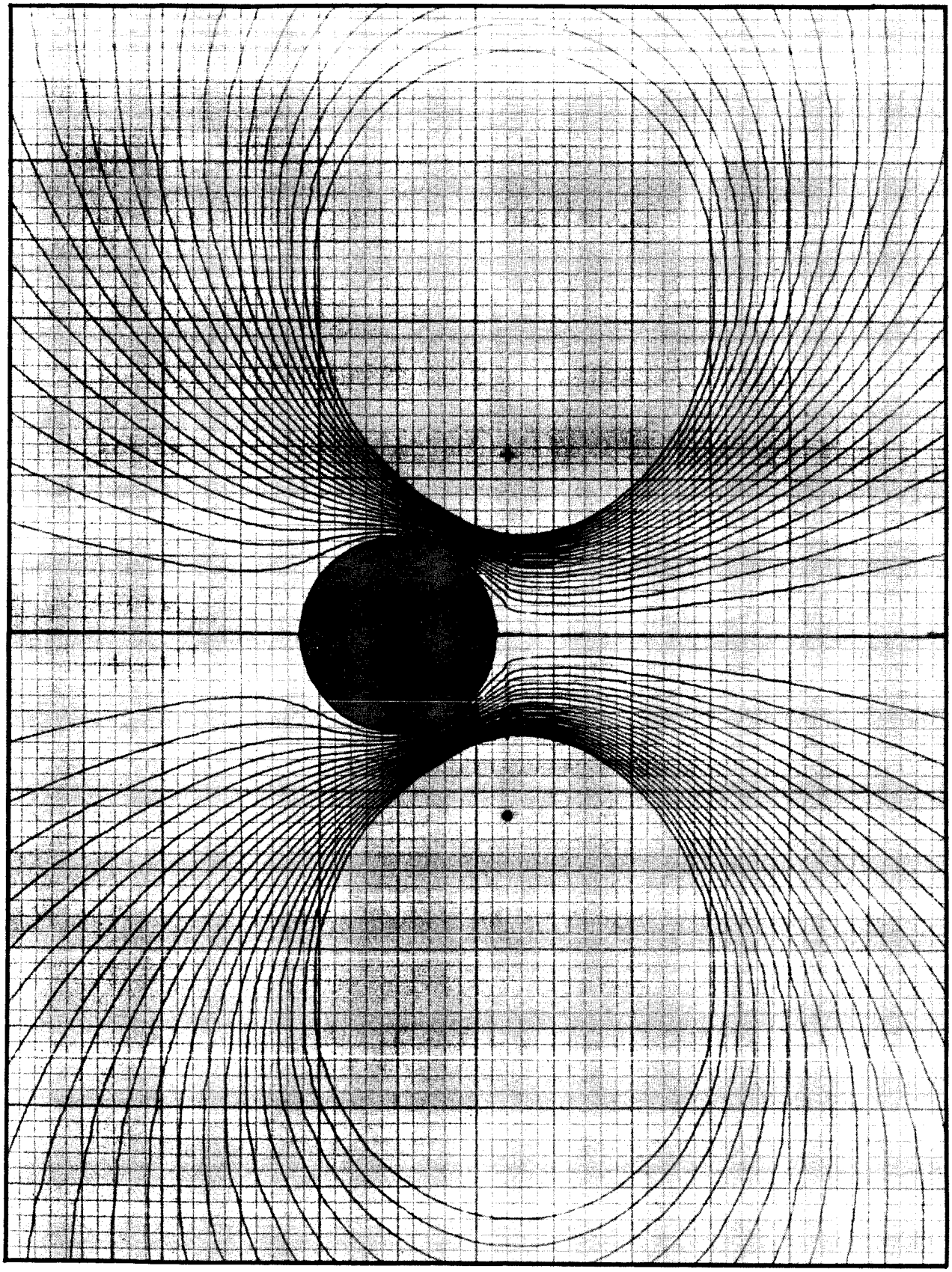

Fig. 1. Effect of superconducting sphere on single-coil field distribution

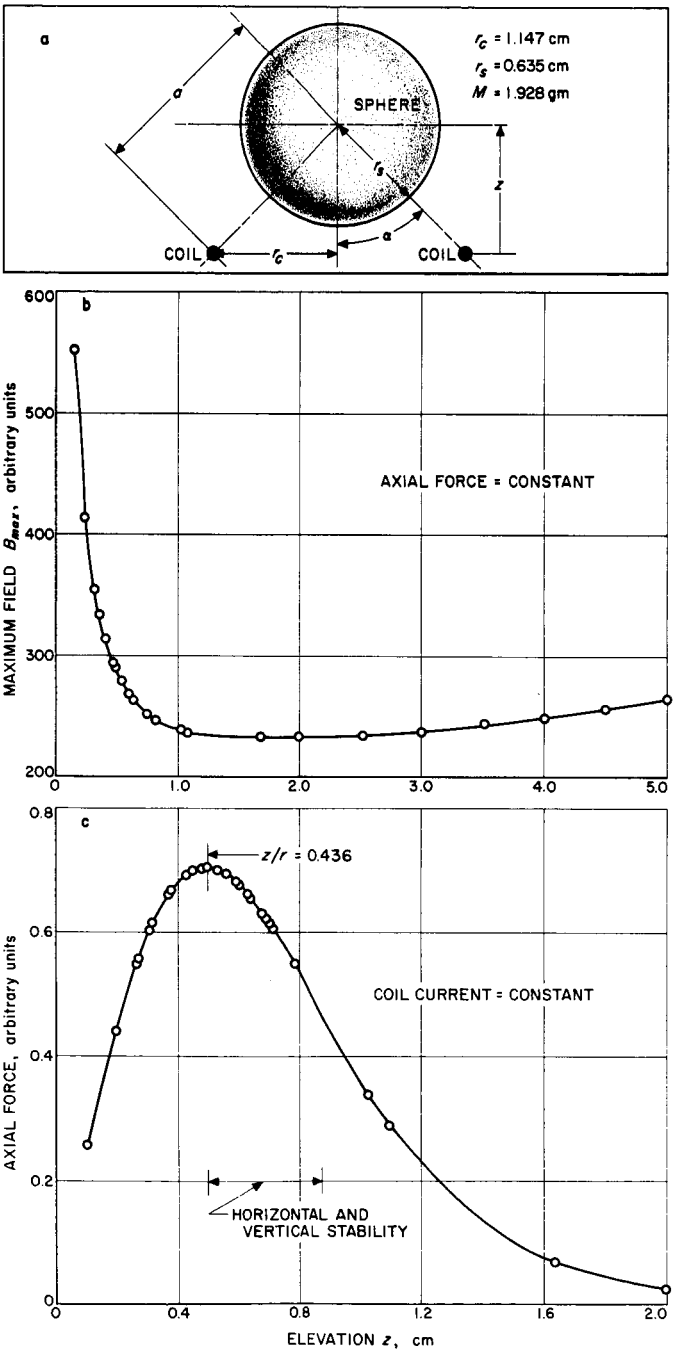

Fig. 2. Geometry and analysis of single-coil configuration

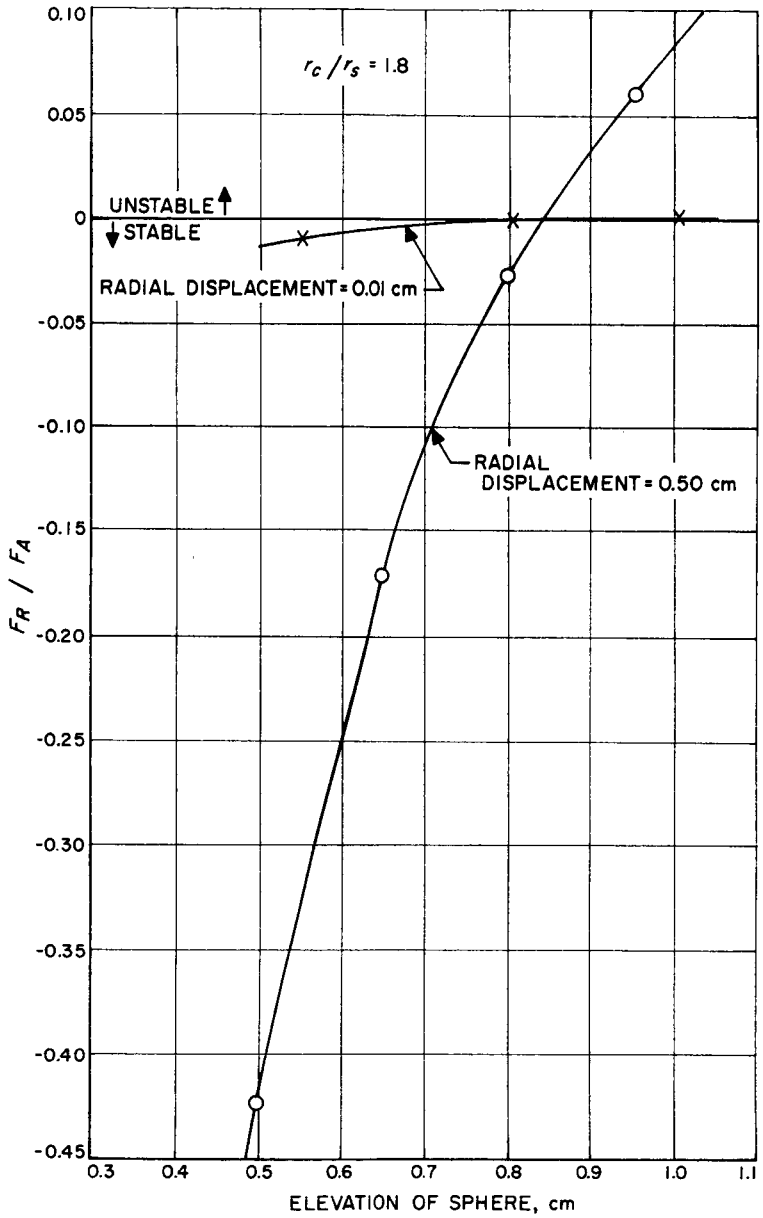

Fig. 3. Radial stability of an off-axis ball levitated by a single coil

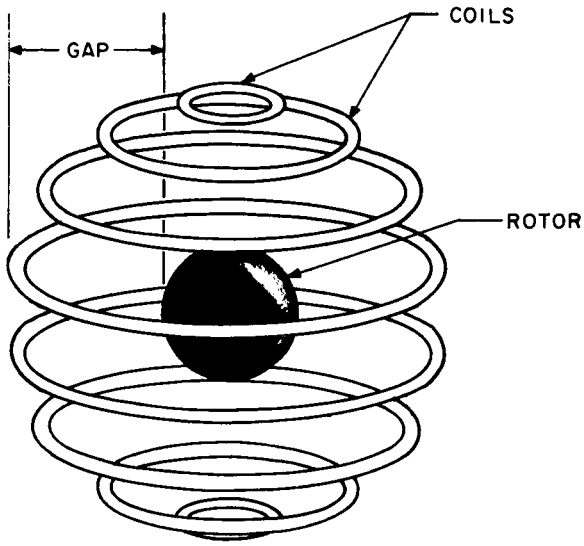

Fig. 4. Eight-coil configuration

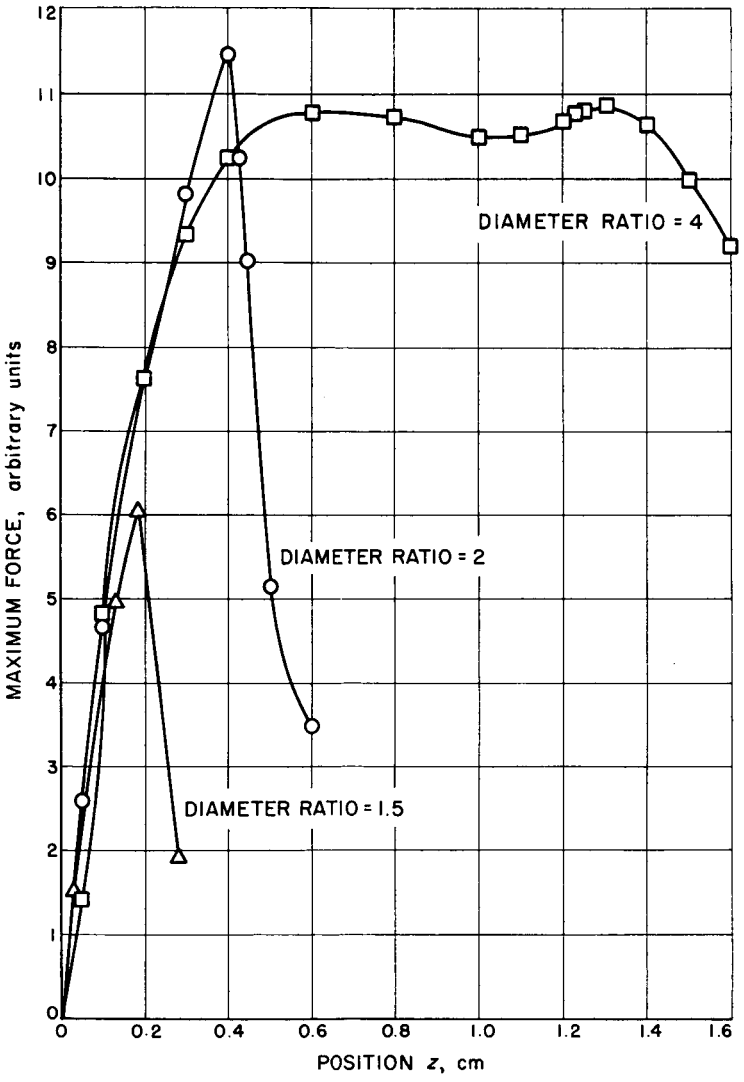

Fig. 5 Effect of gap size on six-coil configuration

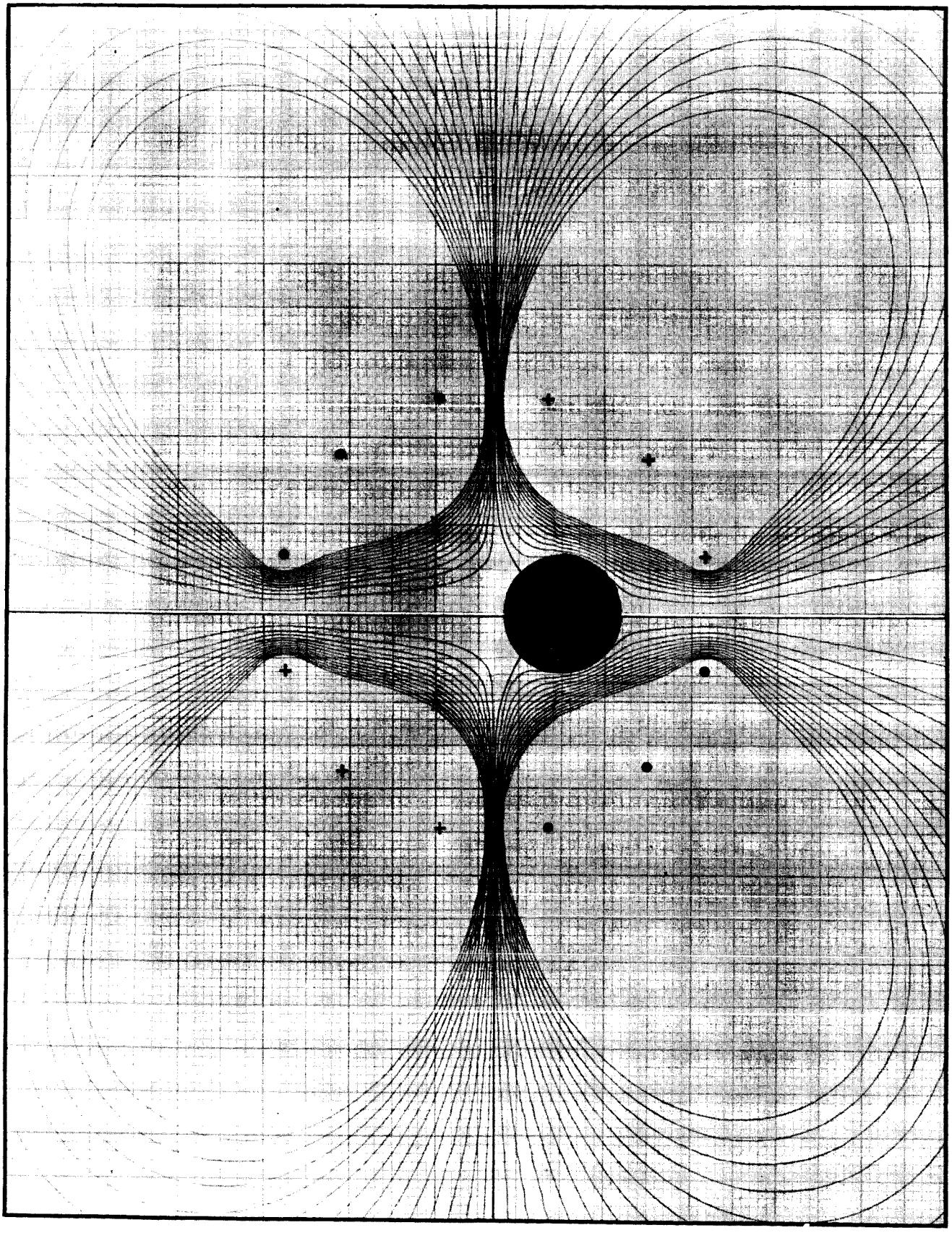

Fig. 6. Effect of superconducting sphere on six-coil field distribution

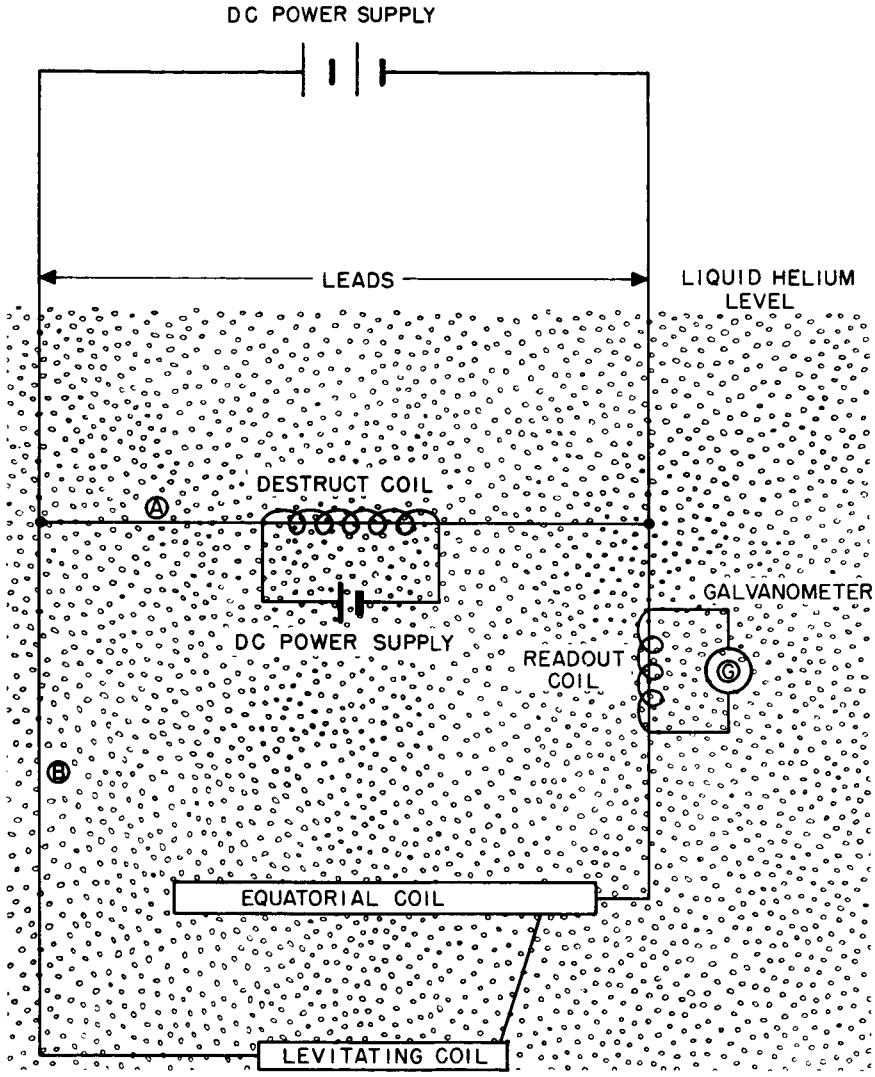

Fig. 7. Block diagram of superconducting loop

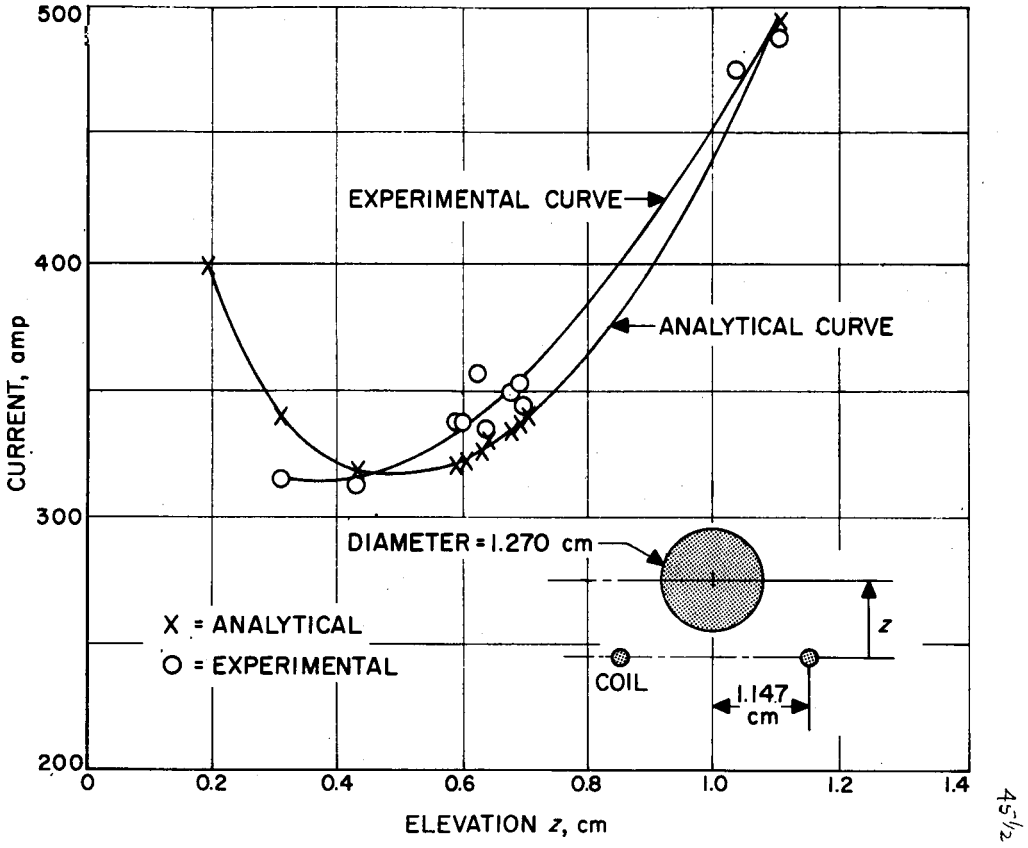

Fig. 8. Analytical and experimental correlation for single coil and sphere (on-axis) configuration

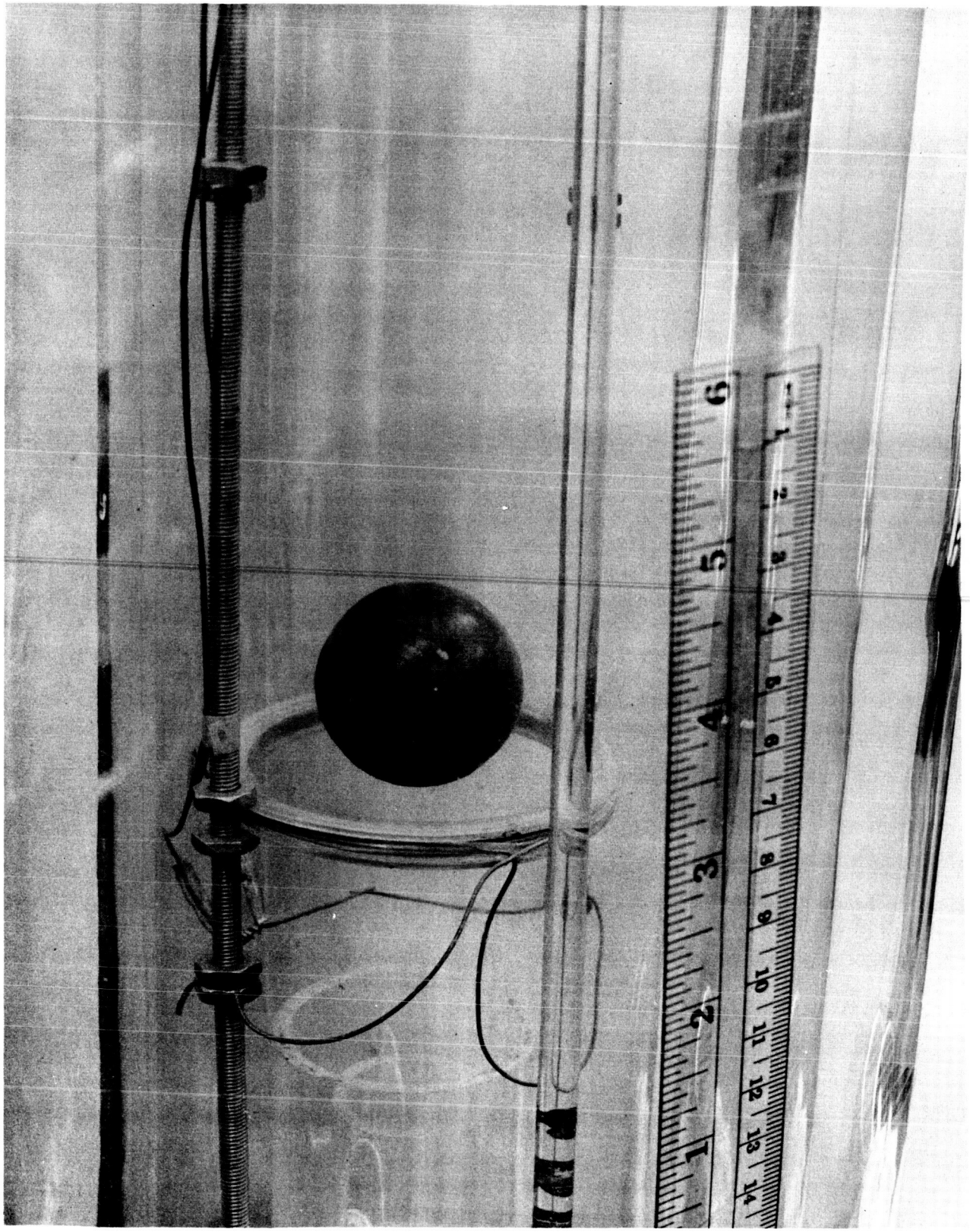

Fig. 9. Experimental single-coil support

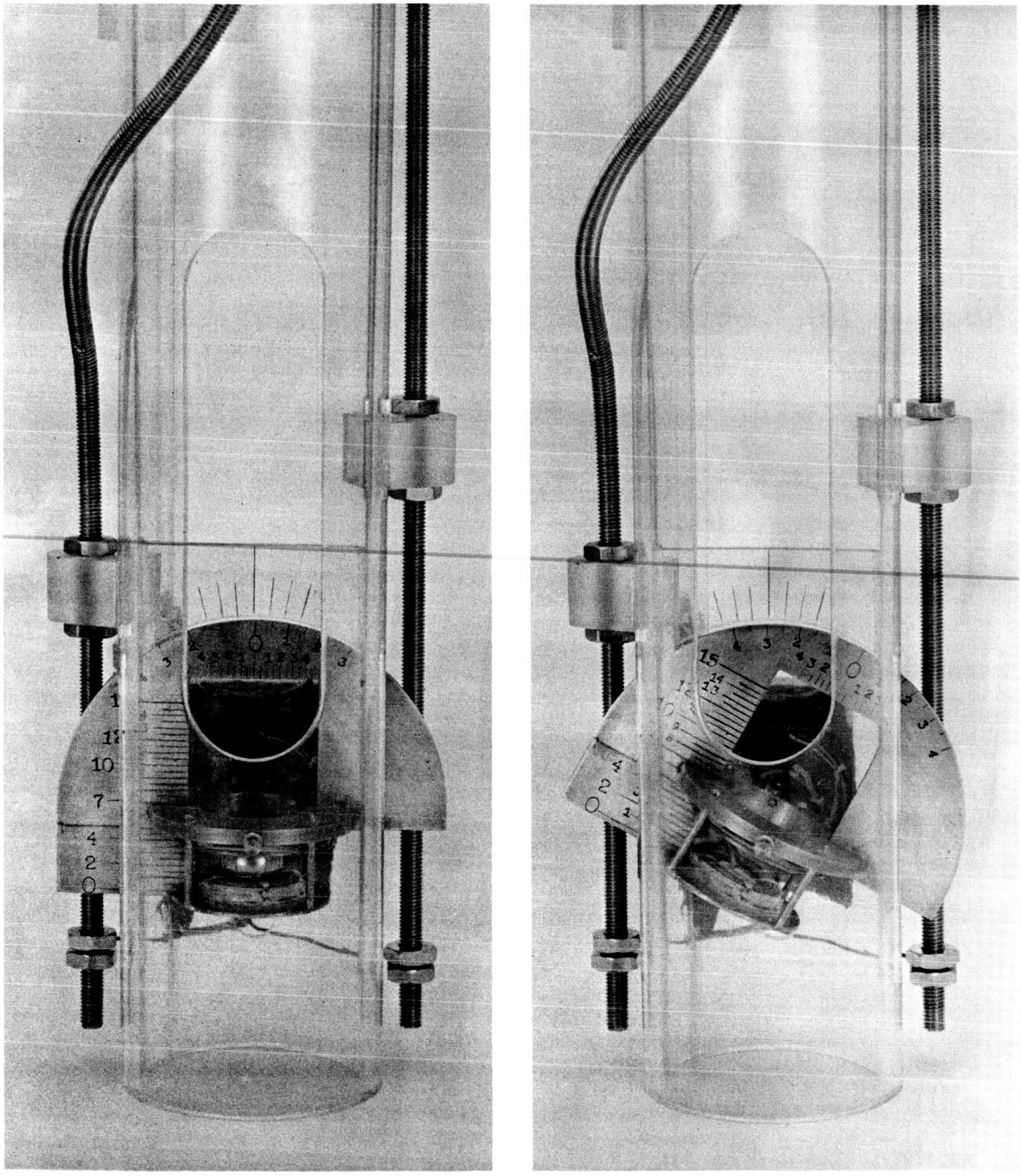

Fig. 10. Apparatus for measuring off-axis forces

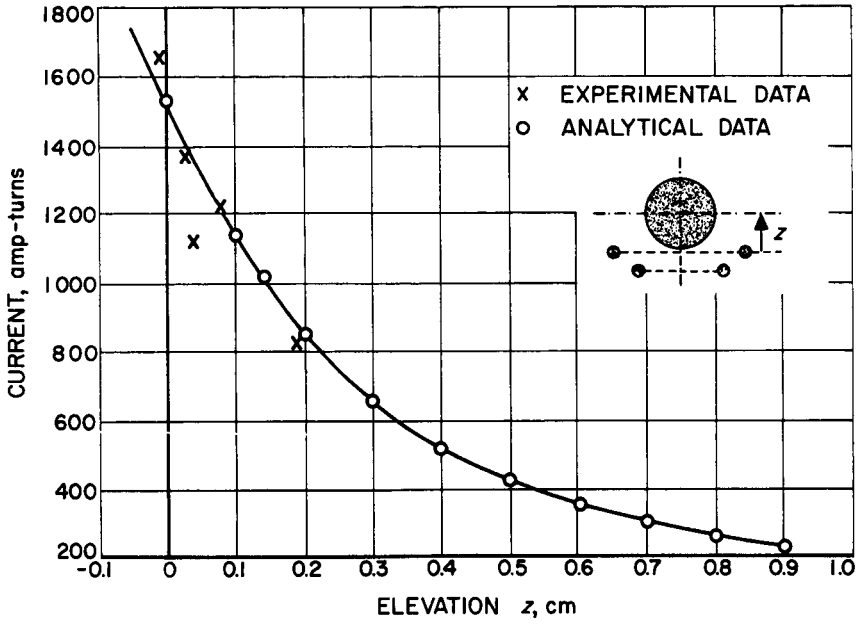

Fig. 11. Analytical and experimental correlation for two-coil (on-axis) configuration

Off-axis two-coil and sphere experimental data

Experimental data				Computed data F_R/F_z	Percentage difference, %
A, cm	Z, cm	θ, deg	tan θ		
0 03	0.05	10	0.18	0.14	22
0.14	0.11	30	0.58	0.45	22
0.13	0 05	20	0.36	0.58	61
0.11	0.17	20	0.36	0.26	28
0.06	0.02	30	0 58	0.26	55

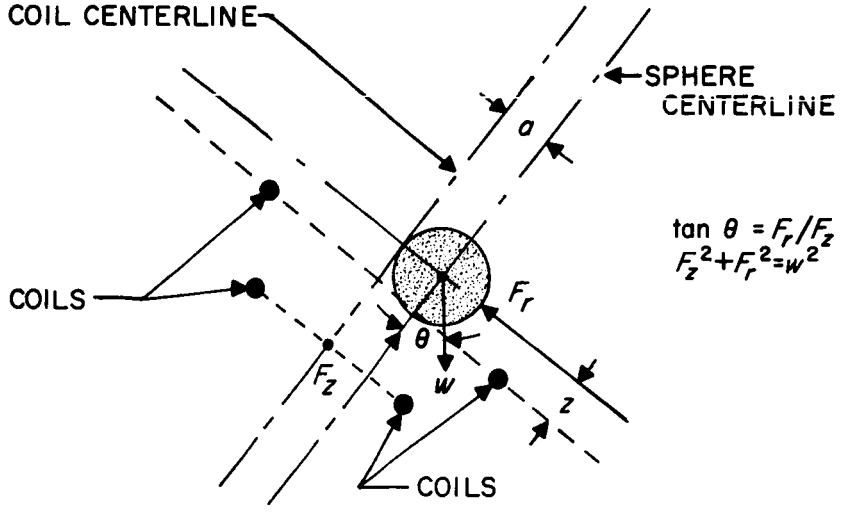

Fig. 12. Off-axis two-coil and sphere configuration

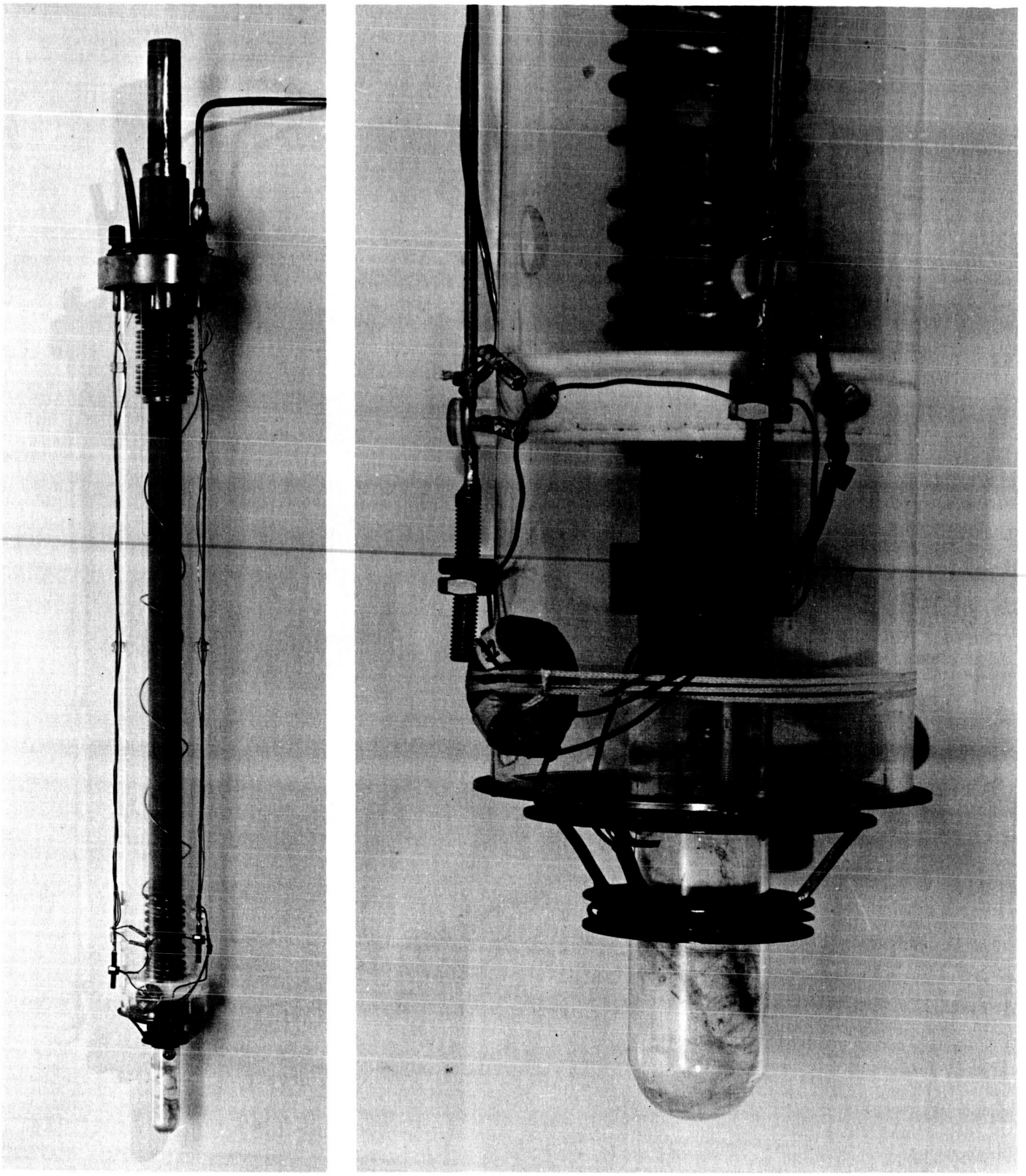

Fig. 13. Levitation in a vacuum

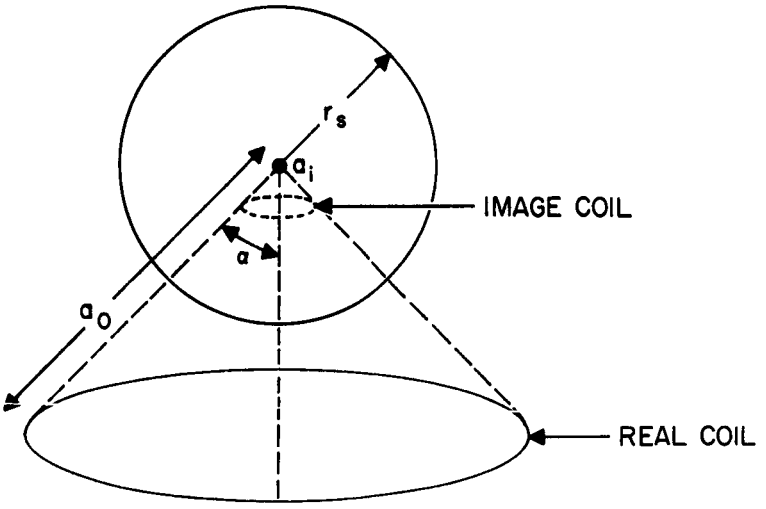

Fig. A-1. Current-loop image in a diamagnetic sphere